MISI-36: Machined image slicer integral field units for the Diffraction-Limited Near-IR Spectropolarimeter

Haosheng Lin[a], Takeshi Sukegawa[b], Morgan Bonnet[a], Yukinobu Okura[b], Tomonao Nakayasu[b], and Yukimasa Suyam[b]

[a]Institute for Astronomy, University of Hawaii, 2680 Woodlawn Drive, Honolulu, HI 96822-1897

[b]Canon Inc., 30-2, Shimomaruko 3-chome, Ohta-ku, Tokyo 146-8501, Japan

ABSTRACT

This paper describes a machined image slicer integral field unit (MISI) for the Diffraction-Limited near-IR Spectropolarimeter (DL-NIRSP) of the Daniel K. Inouye Solar Telescope (DKIST). We have developed and fabricated a prototype machined image slicer IFU (MISI-36) using Canon Inc.'s ultra-high-precision micro-optics fabrication technologies. MISI-36 consists of 112 36μm×1.3mm micro slicer mirrors, a parabolic collimator, a monolithic flat mirror array consists of 112 fold mirrors, and a monolithic spherical mirror array consists of 112 spherical mirrors. This paper provides a brief description of the optical system and preliminary results of laboratory optical performances evaluation of a MISI-36 prototype.

Keywords: Image Slicer, Integral Field Unit, Integral Field Spectrograph, Solar Spectroscopy, Solar Magnetism

1. INTRODUCTION

The Diffraction-Limited near-IR Spectropolarimeter (DL-NIRSP)[1] is one of the first-light facility instruments of the Daniel K. Inouye Solar Telescope (DKIST).[2] DL-NIRSP is equipped with two Birefringent Fiber-Optic Image Slicers (BiFOIS)[3,4] integral field unit (IFU) that allows the instrument to record the spectra from a 2-dimensional field simultaneously. This true-imaging spectroscopic capability will enable observational studies of solar plasma processes with very short dynamic time scale to help advanced the knowledge of the physics of solar plasma processes, and in particular, energetic eruptions such as flares and coronal mass ejections.

With the recent advancement of ultra-high-precision micro-optics fabrication technologies at Canon Inc., it is now possible to fabricate machined image slicers with slicer mirror width of 30 um or less.[5] We have developed a new 36 μm machined image slicer IFU (MISI-36) for DL-NIRSP. MISI-36 is a drop-in replacement and can replace BiFOIS IFU-36 without modifications to DL-NIRSP optical system. This paper briefly describes the optical design of MISI-36. A prototype MISI-36 has been successfully fabricated. This paper will also show preliminary results obtained in the laboratory to assess the performance of MISI-36 prototype. We will also show samples of optical components fabricated with the ultra-high-precision diamond machining process.

2. OPTICAL DESIGN OF DL-NIRSP MACHINED IMAGE SLICER IFU

Figure 1 shows the optical system of MISI-36. This design is constrained by the requirement for MISI-36 to fit into the existing space envelop (70 mm×70 mm×153 mm) of BiFOIS IFU-36. MISI-36 first divide a 2.016 mm×2.664 mm telescope field into 56 36 μm×2.664 mm narrow fields. Each field is further divided into two 36μm×1.332 mm subfields. These 112 subfields are rearranged optically into four segmented and staggered exit slits in the exit port, with 28 subfields within each exit slit.

For each of the micro slicer mirror, the optical system of MISI-36 reimages the micro slicer mirror to a designated position in the exit port using a common parabolic collimator mirror to collimates the diverging

Further author information: (Send correspondence to H.L.)
H.L.: E-mail: haosheng@hawaii.edu, Telephone: 1-808-573-9538

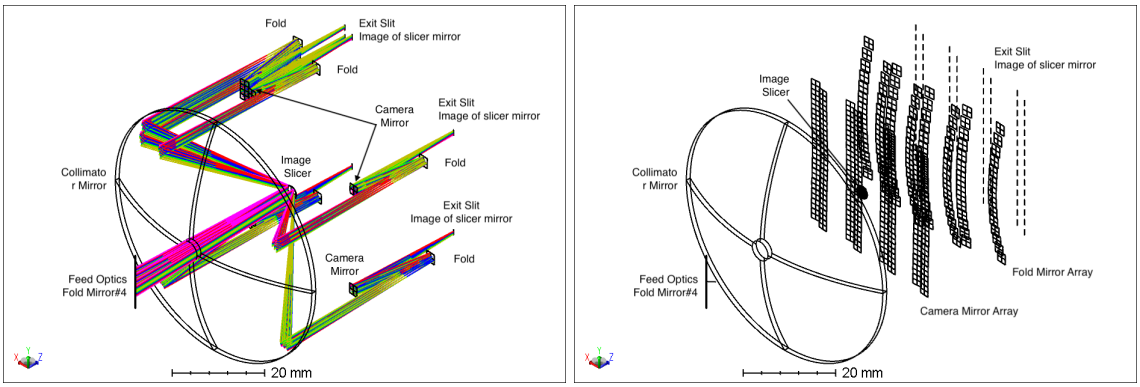

Figure 1. Right Panel: System Diagram of MISI-36. Only the ray traces of 6 out of the 112 micro slicer mirrors are shown to better illustrate the optical configuration of the IFU. Left Panel: The optical system of MISI-36 showing all the optical components and their grouping. Ray traces were turned off to show the optics more clearly.

beam from the slicer mirror, followed by a micro flat folding mirror, and a micro spherical mirror to refocus the image as shown in the left-hand-panel of Figure 1. The optical components of MISI-36 can be grouped into four major components, namely, the Collimator Mirror, the Image Slicer Block, the Spherical Mirror Array, and the Fold Mirror Array (FMA). The right-hand-panel of Figure 1 shows the layout of all optical elements of MISI-36 and the grouping. Ray traces were suppressed to show the optical components and the four major groups more clearly.

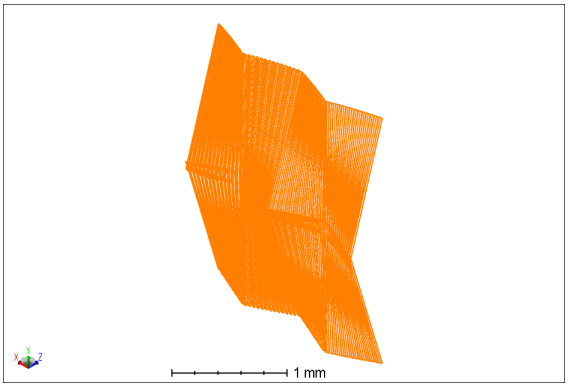

Figure 2. Isometric view of MISI-36 image slicer. The width of the slicer mirrors is 36 μm.

MISI-36 image slicer block consists of 56×2 slicer mirrors, each with a dimension of 0.036 mm×2.664 mm (projected in the focal plane of the telescope) to divide the field into a total of 112 subfields. Figure 2 shows the Zemax 3D model of image slicer block. Similar to the image slicer of the Solar-C project,[5] the multi exit slit configuration of MISI-36 results in the wavy shape of MISI-36. However, due to the constraints of the space available, the "valleys" of the image slicer would have been very deep if the Solar-C image slicer design was used, and renders it unmanufacturable because of tool access issue. For this reason, the MISI-36 image slicer is divided into two sections. This, coupled with the multiple exit slits configuration, resulted in the 2D wavy profiles with a ridge in the center.

The diverging beams reflected by all the slicer mirrors are collimated by the common parabolic mirror with an effective focal length (EFL) of 30 mm. Telescope beam enters the IFU through a center clearance hole of the parabolic mirror. This is another design feature that differ from conventional image slicer IFUs which typically have individually optimized collimating mirror or pupil mirror for each beam. For each micro slicer mirror, a micro fold mirror with a dimension of 2.6 mm×2.2 mm redirects the beam toward a micro spherical mirror with 30 mm focal length to form an image of the subfield at the exit port of the IFU. The dimension of the micro

spherical mirrors is 1.8 mm×2.2 mm. The imaging system has a nominal 1:1 magnification. However, due to the variations in the optical path lengths for each beam, the magnification of the beams vary slightly. The spherical mirrors are approximately one focal length away from the intermediate pupils for each beam formed by the collimator mirror. Therefore, the exit beams are effectively telecentric.

The images of the micro slicer mirrors (equivalently called the micro exit slits) are rearranged into four segmented and staggered exit slits each consists of 28 micro exit slits as shown in the left-hand-panel of Figure 3. The horizontal offset between the 14-segment linear slits are 2.376 mm. The placement of the fold mirrors and camera mirrors as projected in the final exit plane (X-Y plane) of the IFU is shown in the right-hand-panel of Figure 3. The footprint of a H2RG FPA is also shown. The pseudo exit slits position were set to accommodate the anamorphic demagnification of the spectrograph. This results in the two outer-most 14-segment exit slits to be positioned very close to the edge of the H2RG array.

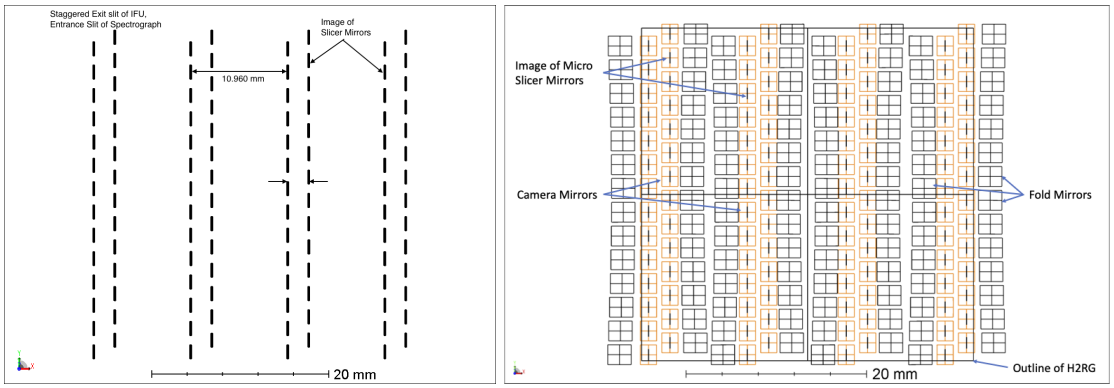

Figure 3. Layout of the fold mirrors and camera mirrors as projected in the plane of the exit slits. The 14 fold mirrors in each of the segmented exit slits are not on a straight line because of the use of a common collimator mirror. The narrow dark lines at the center of the camera mirrors mark the locations of the image of the micro slicer mirrors.

Figure 4 shows the optical configuration of Arm#2 of DL-NIRSP spectrograph integrated with MISI-36. MISI-36 is uses a 6-mirror 1:1 reimaging system composed of two identical off-axis parabola, and four fold mirrors. The distance between the entrance focal plane of the relay system to the nominal exit slit plane of MISI is set to 153 mm to match the length of BiFOIS IFUs. DL-NIRSP is equipped with a Richardson Grating 23.2 line/mm R2 grating with a ruled area of 300 mm×150 mm and a blazing angle of 63.5 deg. The nominal spectrograph angle (grating $\alpha - \beta$) is 4.9 deg, which varies depends on the spectral lines are observed. The nominal anamorphic demagnification of the spectrograph is 0.68. This reduces the distances between the pseudo exit slits and place the spectral images mostly within the size limit of the H2RG array.

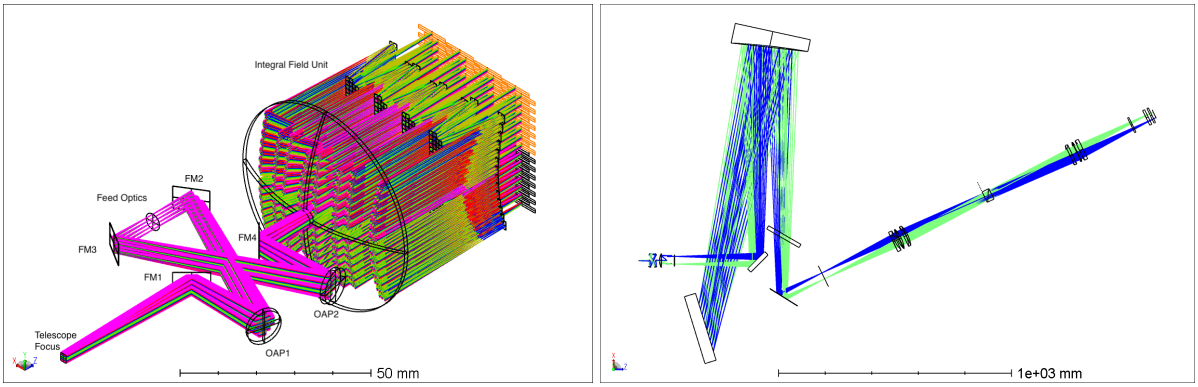

Figure 4. Left: Full Zemax model of MISI-36, including a 1:1 relay optics. Right: Model of DL-NIRSP spectrograph with MISI-36 upgrade for Spectral Arm#2. Only ray traces of slicer mirror#1 (green) and #56 (blue) are shown.

MISI-36 will be used with the F/62 and F/24 feed optics of DL-NIRSP. However, the fold mirrors and camera mirrors were oversized for a F/15 beam in the spectral direction to accommodate the expected broadening of the beams due to slit diffraction. The through-focus spot diagram of the first and last slicer mirror (Configuration 1 and 56) are shown in Figure 5. The image quality of Configuration 56 is worse than that of Configuration 1 because of the beams of Configuration 56 falls closer to the edge of the off-axis collimator/camera mirror of the spectrograph. This is the expected behavior of the off-axis Littrow spectrograph. The worst spot size of Configuration 56 of 21 μm is well below the 36 μm spatial sampling size of the IFU.

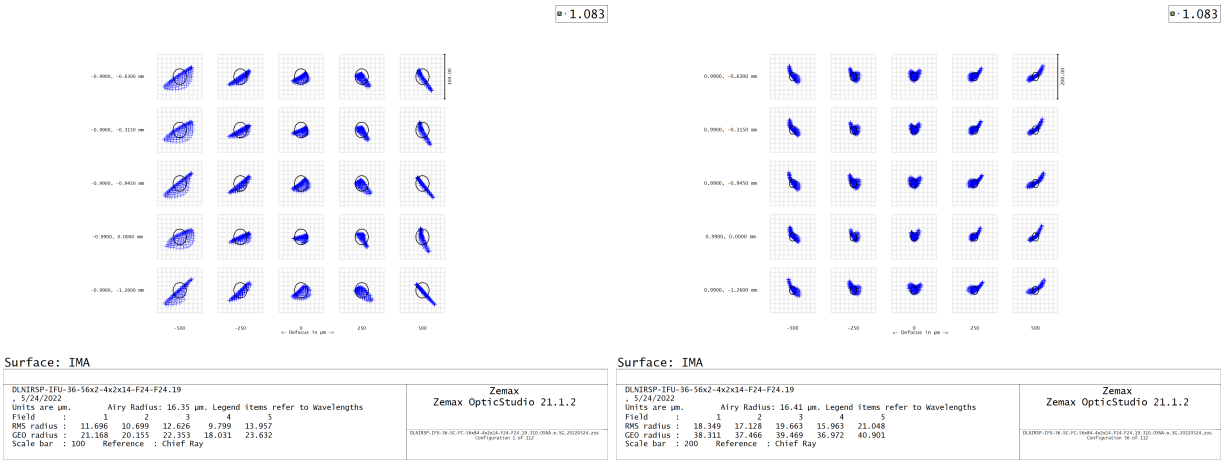

Figure 5. Through-focus spot diagram of the first slit (Configuration 1, left hand panel) and last slit (Configuration on 56, right hand panel), respectively.

3. THE MECHANICAL SYSTEM OF MISI-36

There are a total of 449 optical mirrors in the optical system of MISI-36. Given the clustering of the fold mirrors and camera mirrors in the optical path, MISI's mechanical design groups the optical components into five major mechanical sub-components, namely, 1) the image slicer block; 2) the collimator mirror; 3) the fold mirror array; 4) the camera mirror array, and 5) the exit field stop in the order along the optical path. Tolerance analysis showed that a positional error (X and Y decenter) of ± 50 μm and a pointing error (tip/tilt) of ± 0.05 degree for the optical components of the image slicers do not introduce noticeable performance degradation of the DL-NIRSP spectrograph. Canon's ultra-high-precision diamond cutting technology is capable of fabricating complex micro structures on a large monolithic substrate with better than $\pm 1 \mu$m positional and dimensional accuracy, and ± 0.001 degree pointing accuracy globally. Therefore, precise alignment of the MISI-36 optical system can be achieved with constraints in the MISI-36 mechanical design to ensure precise positioning and angular alignment between the four sub-components in the final IFU assembly. Fig. 6 shows CAD (computer-added design) rendering of the MISI-36 assembly and its major components. A scanning electron microscope (SEM) image of the as-built image slicer is shown also, demonstrating the diamond cutting CNC mill's ability to produce the complex optical structure with high precision.

4. PRELIMINARY PERFORMANCE EVALUATION OF MISI-36 PROTOTYPE

Evaluation of the efficiency, spatial and spectral resolution, and scattered light performance of MISI-36 prototype was performed in the Maui laboratory of the Institute for Astronomy (IfA) or the University of Hawaii.

Efficiency The left hand panel of Fig. 7 shows the experimental setup for the measurement of MISI-36 efficiency. The mirrors of MISI-36 are coated with a protective silver coating. However, the side walls of the image slicer cause shadowing and can reduce the efficiency of the IFU. The photon transfer efficiency ε of MISI-36 was measured using a supercontinuum laser (SCL) with a 1.2 mm diameter collimated output beam to illuminate the image slicer block. An 8" integration sphere with a 40 mm aperture captures all the output beams of the

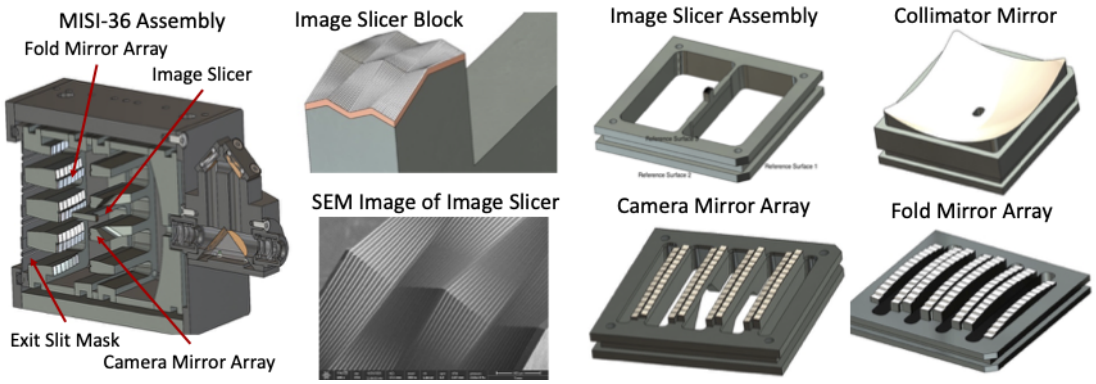

Figure 6. CAD models of MISI-36 Assembly, its major components, and a SEM image of the image slicer.

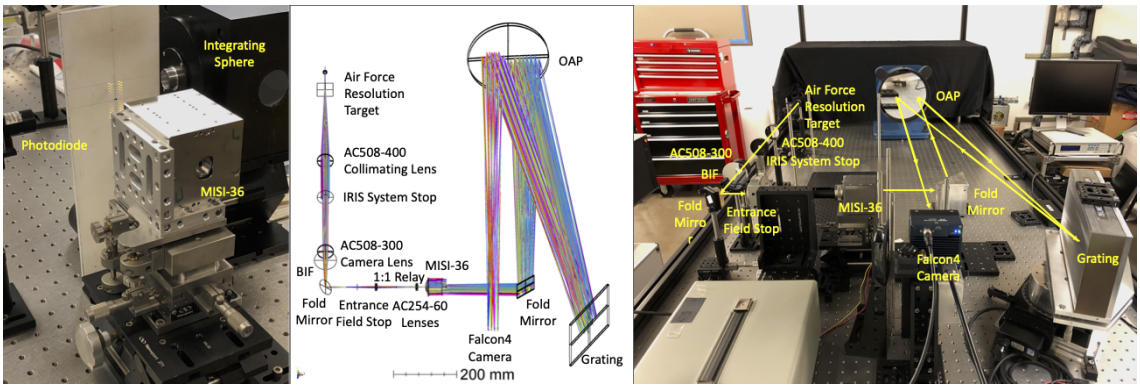

Figure 7. **(Left)** Picture of MISI-36 and the integrating sphere used for the efficiency measurement. The output beams of the center section of the image slicer block illuminated by a supercontinuum laser can be seen on the white screen. **(Middle)** Zemax optical model of the setup for spatial and spectral resolution evaluation. **(Right)** Picture of the experimental setup. Yellow lines indicate the beam path.

IFU. A silicon photometer was used to measure the intensity at the output port of the integration sphere. The ratio of the intensities with direct illumination by the SCL and that by the output of MISI-36 yields ε=70%.

Spatial Resolution The center and right-hand panel of Figure 7 show the experimental setup for the evaluation of the spatial and spectral resolution of MISI-36. The test system includes a 4:3 relay system to image an Air Force resolution target on the entrance field stop of another 1:1 relay into MISI-36 image slicer, and an off-axis reflecting Littrow spectrograph with a 79 line/mm R2 eschelle grating simular the spectrograph of DL-NIRSP. A Teledyne Falcon4 CMOS camera was used to record the spectra. The right-hand panel of Fig. 8 shows a sample Air Force resolution target spectral image of the Fe I 630 nm lines obtained with this setup. Three region of interests (ROIs) and their close ups are marked by the small yellow rectangular boxes. The intensity plot of ROI#3 in the upper panel of the middle column shows that two horizontal bars (located between pixel 25 and 40) separated by about 10 pixels (60 μm) are resolved according to Rayleigh's Criterion, demonstrating the experimental setup's spatial resolution along the slit's long direction.

Spectral Resolution The spectral resolution of MISI-36 near 630 nm wavelength band was measured to be $\lambda/\Delta\lambda_{FWHM} = 250,000\lambda/\Delta\lambda_{FWHM} = 250,000$ measured from the spectra of a HeNe 632.8 nm laser. The lower panel of the middle column of Fig. 8 shows an integrated sunlight Fe I 630 nm line spectra obtained with MISI-36, and the National Solar Observatory (NSO) Fourier Transform Spectrograph (FTS) reference spectra from the McMath-Pierce Solar Telescope at Kitt Peak. The spectral line depth and width of the MISI-36 Fe I 630.1 nm line are shallower and broader than those of the FTS spectrum as expected, but are comparable to the Hinode Spectropolarimeter.[6]

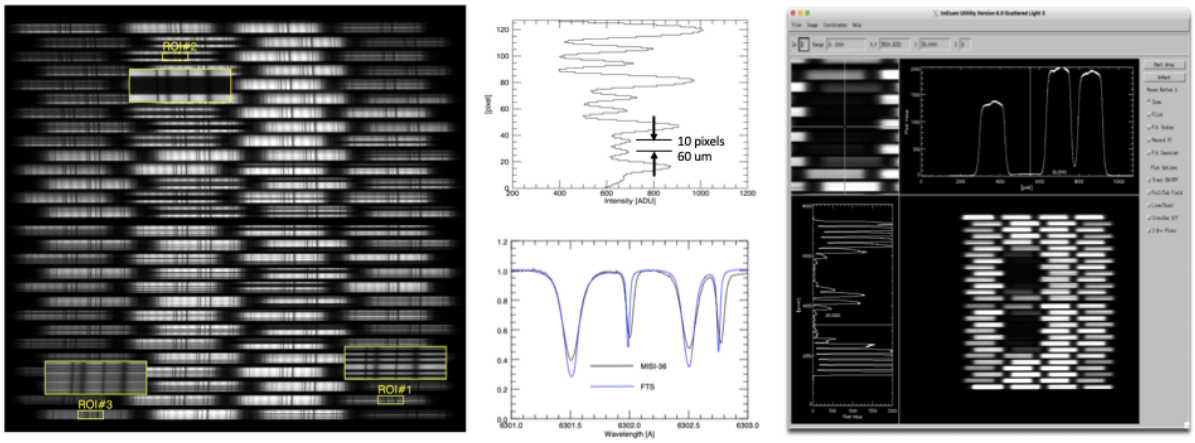

Figure 8. **(Left)** Spectral image of an Air Force resolution target illuminated by integrated sunlight at the Fe I 630 nm wavelength. **(Middle Upper Panel)** Vertical intensity profile of ROI#3. Features separated by 60 μm are resolved. **(Middle Lower Panel)** Fe I 630 nm lines spectra from MISI-36 and Kitt Peak FTS. **(Right)** MISI-36 spectra shadowed by a copper wire for scattered light measurements. Intensity in the darkest areas in the 2^{nd} column from the left of the spectral image are used to evaluate the scattered light of the system.

Scattered Light The scattered light in MISI-36 was evaluated using a 250μm diameter copper wire placed at the entrance field stop to cast a shadow in the spectral image, as shown in the right panel of Fig. 8. The amplitude of the scattered light as measured from the intensity at the center of the shadowed areas is 2% of that of the fully illuminated spectrum. Since this measurement includes contribution from the spectrograph, the 2% figure is considered the upper limit of the scattered light caused by MISI-36.

Image Reconstruction Figure 9 shows an reconstructed image of the AF Resolution Target. Only edge detection algorithm was used to find the (spatial) edges of the spectra, and a 1:1 magnification of the slicer mirror images was assumed. A more elaborated knife-edge scanning calibration method[3] will be used to generate the correct mapping of the telescope focal plane.

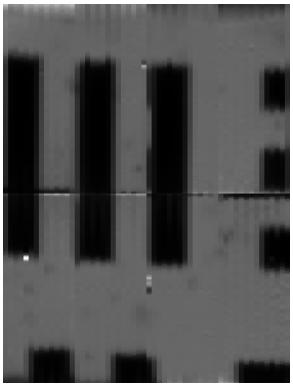

Figure 9. An image of a small section of the Air Force resolution target obtained with MISI-36 test spectrograph using a preliminary data descrambling routine. The format of the image is 56×72 pixels with a pixel size of 36 μm defined by the slicer mirror width.

5. SUMMARY

This paper describes the design of a machined image slicer IFU for integral field spectroscopy. A prototype device has been successfully fabricated and tested. Preliminary evaluation showed that the MISI performed as

expected and yield high spectral and spatial resolution. A new MISI-36 IFU for DL-NIRSP upgrade is now under construction. It will be commisioned in the first quarter of 2023.

ACKNOWLEDGMENTS

This research was partially supported by an NSF MRI award 1727095. The fabrication of the MISI-36 prototype was funded by Canon internal funding.

REFERENCES

[1] Jaeggli, S. A., Lin, H., Onaka, P., Yamada, H., Anan, T., Bonnet, M., Ching, G., Huang, X.-P., Kramar, M., McGregor, H., Nitta, G., Rae, C., Robetson, L., Schad, T. A., Toyama, P., Young, J., Berst, C., Harrington, D. M., Liang, M., Puentes, M., Sekulic, P., Smith, B., and Sueoka, S. R., "The Diffraction-Limited Near-IR Spectropolarimeter (DL-NIRSP) of the Daniel K. Inouye Solar Telescope (DKIST)," **295**, 172 (Dec. 2022).

[2] Rimmele, T. R., Warner, M., Keil, S. L., Goode, P. R., Knölker, M., Kuhn, J. R., Rosner, R. R., McMullin, J. P., Casini, R., Lin, H., Wöger, F., von der Lühe, O., Tritschler, A., Davey, A., de Wijn, A., Elmore, D. F., Fehlmann, A., Harrington, D. M., Jaeggli, S. A., Rast, M. P., Schad, T. A., Schmidt, W., Mathioudakis, M., Mickey, D. L., Anan, T., Beck, C., Marshall, H. K., Jeffers, P. F., Oschmann, J. M., Beard, A., Berst, D. C., Cowan, B. A., Craig, S. C., Cross, E., Cummings, B. K., Donnelly, C., de Vanssay, J.-B., Eigenbrot, A. D., Ferayorni, A., Foster, C., Galapon, C. A., Gedrites, C., Gonzales, K., Goodrich, B. D., Gregory, B. S., Guzman, S. S., Guzzo, S., Hegwer, S., Hubbard, R. P., Hubbard, J. R., Johansson, E. M., Johnson, L. C., Liang, C., Liang, M., McQuillen, I., Mayer, C., Newman, K., Onodera, B., Phelps, L., Puentes, M. M., Richards, C., Rimmele, L. M., Sekulic, P., Shimko, S. R., Simison, B. E., Smith, B., Starman, E., Sueoka, S. R., Summers, R. T., Szabo, A., Szabo, L., Wampler, S. B., Williams, T. R., and White, C., "The Daniel K. Inouye Solar Telescope - Observatory Overview," **295**, 172 (Dec. 2020).

[3] Lin, H. and Versteegh, A., "VisIRIS: a visible/IR imaging spectropolarimeter based on a birefringent fiber-optic image slicer," in [*Society of Photo-Optical Instrumentation Engineers (SPIE) Conference Series*], McLean, I. S. and Iye, M., eds., *Society of Photo-Optical Instrumentation Engineers (SPIE) Conference Series* **6269**, 62690K (June 2006).

[4] Schad, T., Lin, H., Ichimoto, K., and Katsukawa, Y., "Polarization properties of a birefringent fiber optic image slicer for diffraction-limited dual-beam spectropolarimetry," in [*Ground-based and Airborne Instrumentation for Astronomy V*], Ramsay, S. K., McLean, I. S., and Takami, H., eds., *Society of Photo-Optical Instrumentation Engineers (SPIE) Conference Series* **9147**, 91476E (Aug. 2014).

[5] Suematsu, Y., Sukegawa, T., Okura, Y., Nakayasu, T., Enokida, Y., Koyama, M., Saito, K., Ozaki, S., and Tsuneta, S., "Development of micro image slicer of integral field unit for spaceborne solar spectrograph," in [*Advances in Optical and Mechanical Technologies for Telescopes and Instrumentation*], Navarro, R., Cunningham, C. R., and Barto, A. A., eds., *Society of Photo-Optical Instrumentation Engineers (SPIE) Conference Series* **9151**, 91511S (July 2014).

[6] Lites, B. W., Akin, D. L., Card, G., Cruz, T., Duncan, D. W., Edwards, C. G., Elmore, D. F., Hoffmann, C., Katsukawa, Y., Katz, N., Kubo, M., Ichimoto, K., Shimizu, T., Shine, R. A., Streander, K. V., Suematsu, A., Tarbell, T. D., Title, A. M., and Tsuneta, S., "The Hinode Spectro-Polarimeter," **283**, 579–599 (Apr. 2013).